Pharm Res (2010) 27:1103–1114
DOI 10.1007/s11095-010-0054-5

RESEARCH PAPER

Anti-Melanoma Effects of Vorinostat in Combination with Polyphenolic Antioxidant (−)-Epigallocatechin-3-Gallate (EGCG)

Minakshi Nihal • Craig T. Roelke • Gary S. Wood

Received: 20 October 2009 / Accepted: 5 January 2010 / Published online: 16 March 2010

ABSTRACT

Purpose Melanoma is an aggressive neoplasm with a propensity for metastases and resistance to therapy. Previously, we showed that (-)-epigallocatechin-3-gallate (EGCG), the major polyphenolic antioxidant present in green tea, resulted in a significant decrease in the viability and growth of melanoma and induction of apoptosis via modulation of the cki-cdk-cyclin network and Bcl2 family proteins. Epigenetic regulation of gene transcription by histone deacetylase (HDAC) inhibitors is gaining momentum as a novel cancer therapy. SAHA-suberoylanilidine hydroxamic acid Zolinza® (vorinostat) is the first HDAC inhibitor approved by the U.S. FDA. In this study, we determined if vorinostat alone or in combination with EGCG imparts anti-proliferative effects against human melanoma cells.

Methods Employing human melanoma cell lines A-375, Hs-294T and G-361, we determined the effect of vorinostat and/or EGCG on 1) growth/viability and colony formation, 2) apoptosis, and 3) the critical molecules involved in cell cycle and apoptosis regulation.

Results Our data demonstrated that the anti-proliferative effects of vorinostat were greater than or similar to those of EGCG among the cell lines tested. Furthermore, relative to monotherapy, the combination treatment resulted in significantly greater inhibition of cell proliferation, increased apoptosis, activation of p21, p27 and caspases (3, 7 and 9) and Bax as well as down-regulation of cdk2, cdk4, cyclin A, NF-κB protein p65/RelA and Bcl2 protein and transcript.

Conclusions Our preclinical findings suggest that combination therapy with EGCG and vorinostat may be beneficial for the management of human melanoma.

KEY WORDS chemoprevention · EGCG · green tea · melanoma · vorinostat

INTRODUCTION

Melanomas are infamous for their resistance to treatment-induced apoptosis, thereby imparting them with a selective advantage for progression and metastasis (1). Chemoprevention of melanoma is an underdeveloped area of research that could potentially complement ongoing prevention and treatment strategies (2,3). The major polyphenolic constituent of green tea, (−)-epigallocatechin-3-gallate (EGCG), has been shown to impart anti-proliferative and chemopreventive effects against several cancers, including skin cancer (4). We demonstrated previously that EGCG treatment of melanoma cells results in cell cycle blockade and induction of apoptosis via modulation of the cki-cyclin-cdk network and Bcl2 family proteins (5). We also showed that EGCG can enhance the therapeutic response of melanoma to IFN-alpha both *in-vitro* and in nude mouse xenografts (6).

Histone deacetylase (HDAC) inhibitors are a novel class of small molecules being evaluated as epigenetic regulators of gene transcription in clinical trials for a number of different malignancies (7,8). HDAC inhibitors have been associated with a variety of diverse molecular and biological

Supported by Merit Review funding from the Department of Veterans Affairs and Merck & Co, Boston, Massachusetts, USA.

Electronic supplementary material The online version of this article (doi:10.1007/s11095-010-0054-5) contains supplementary material, which is available to authorized users.

M. Nihal · C. T. Roelke · G. S. Wood
Department of Dermatology, University of Wisconsin School of Medicine and Public Health
1300 University Avenue, Room B25
Madison, Wisconsin 53706, USA

G. S. Wood (✉)
Wm. S. Middleton VA Medical centre
Madison, Wisconsin, USA
e-mail: gwood@dermatology.wisc.edu

effects, ranging from transcriptional control, chromatin remodeling, protein–DNA interaction, cellular differentiation, growth arrest and apoptosis (9). One current area of interest is the design of combination protocols aimed at enhancing HDAC inhibitor efficacy (10).

Zolinza® (vorinostat) is the first HDAC inhibitor approved by the FDA. It is indicated for the treatment of cutaneous T-cell lymphoma, which exhibits a response rate of about 30% (11). Phase IIb multicenter trial of vorinostat in patients with persistent, progressive, or treatment refractory cutaneous T-cell lymphoma concluded with effective treatment in refractory MF/SS with an acceptable safety profile (12). Phase I and Phase II trials of vorinostat in multiple myeloma (13), diffuse large B-cell lymphoma (14), ovarian carcinoma (15) and acute myeloid leukemia (16) resulted in modest to minimal activity as a single agent. Vorinostat in combination with other agents, such as radiation therapy and chemotherapy, might have synergistic or additive effects in a variety of cancers (8,17–19). In this study, we tested the effects of vorinostat alone and in combination with EGCG against human melanoma.

MATERIAL AND METHODS

Cell Culture and Treatment

The melanoma cells were obtained from The American Type Culture Collection (ATCC, VA) and were maintained at standard tissue culture conditions as recommended by the vendor. Vorinostat (Merck & Co., NJ) was dissolved in DMSO. EGCG was obtained from Sigma-Aldrich Co. and dissolved in PBS and added to the growth medium.

Trypan Blue Exclusion Assay

After trypsinization, untreated and treated cells were pelleted by centrifugation and re-suspended in PBS (1 mL). Trypan blue (10 μL) was added to a smaller aliquot (10 μL) of cell suspension, and the number of cells (viable-unstained and non-viable-blue) was counted. Viability was expressed as the percent viable cells out of the total number of cells. Cell growth data were analyzed as percent change of total cell numbers between treatments. The (*) represents statistically significant change compared to vehicle controls (no treatment = NT), compared to EGCG (!) and vorinostat (^).

Colony Formation Assay

A-375, Hs-294T and G-361cells were plated in triplicate on a 6-well tissue culture plate (1, 4, 5×10^3 cells/well). The control and treated cells were cultured for 7–15 days (7 days for A-375 due to high growth) with growth media replaced every 3 days. The cells were then stained with crystal violet (a formulation of 1:2:2 of methanol: water: 0.1% crystal violet in acetic acid) washed with PBS and air-dried. The colonies were counted arbitrarily, and thereafter plates were scanned for photograph.

Annexin V Binding Assay

Control and treated cells were trypsinized, collected and washed with PBS. Cells were then resuspended in 100 μl binding buffer (0.1 M Hepes, pH 7.4; 1.4 M NaCl; 25 mM $CaCl_2$) and stained with FITC-conjugated Annexin V antibody and propidium iodide (BD Biosciences, CA) as per vendor's suggestions. The cells were then analyzed on a FACScan benchtop cytometer at the UWCCC Flow cytometry facility, and further analysis was performed with CellQuest software/FlowJo software (BD Biosciences, CA/ Treestar, OR).

Quantitative Real Time PCR (QRT-PCR)

Briefly, cells (70–80% confluency) were treated for 48 h, washed with DEPC water and pelleted. The cell pellet was resuspended in Trizol reagent (Invitrogen Corporation, CA), and RNA was extracted according to the vendor's recommendation. RNA was treated with DNAse (Invitrogen Corporation, CA), and first-strand cDNA was transcribed with 500 ng oligo dT primers, 10 mM dNTPs and 200 units of M-MLV reverse transcriptase (Invitrogen Corporation, CA). Quantitative real time (QRT-PCR) was performed in triplicate with SYBR® Premix ExTaq (Takara Bio USA, WI) with 50 ng first strand cDNA, 0.2 μM each for Bcl2 forward (5′-CATGTGTGTGGAGAGCGTCAA-3′) and reverse (5′ACAGTTCCACAAAGGCATCCC-3′) primers and GAPDH forward (5′-GGGTGTGAACCATGAGAAGT-3′) and reverse (5′-GTAGAGGCAGGGATGATGTT-3′) primers. The samples in triplicate were cycled once for 94°C for 2 min then 40 cycles of 94°C; 15 s, 58°C; 30 s, 72°C; 45s each. Relative Bcl2 mRNA was calculated using the ΔΔCT comparative method using GAPDH as an endogenous control and NT controls as the calibrator.

Protein Lysates and Western Blot Analysis

Following treatment, cells were trypsinized, washed with ice-cold PBS, collected by centrifugation and lysed in lysis buffer containing protease inhibitors (50 mM Tris, 150 mM NaCl, 1% NP-40, 0.5% deoxycholic acid, 0.1% SDS) with phenylmethylsulphonyl fluoride (PMSF) and protease inhibitor cocktail (Pierce, IL). The cell suspension was cleared by centrifugation at 14,000 × g for 20 min at 4°C, and the supernatant (whole cell lysate) was collected. The protein

concentration was determined using the BCA Protein Assay (Pierce, IL).

For immunoblot analysis, 20–50 μg protein was subjected to SDS-PAGE, transferred onto a nitrocellulose membrane and blocked with TBST plus 5% dry milk and probed with an appropriate primary antibody followed by a secondary HRP-conjugated antibody. The protein was detected by chemiluminescence. Blots were subsequently stripped and re-probed with goat anti-β-actin (Santa Cruz, CA) primary antibody followed by appropriate secondary and chemiluminescent detection as a loading control. The quantification of protein was performed by digital analyses of protein bands (TIFF images) using UN-SCAN-IT software (Silk Scientific, Inc., UT).

Immunofluorescence Staining

For immunofluorescence staining, the cells were plated and grown on BD Falcon CultureSlides (BD Biosciences, CA) and treated with EGCG (10 μg/mL), vorinostat (1 μM) and combination. After 48 h post-treatment, cells were fixed with 100% methanol and permeabilized with 0.5% Triton-X 100 in PBS and then blocked for 1 h at room temperature in 10% normal goat serum in PBS. Following blocking, biotin-conjugated mouse Ki-67 (FITC) or anti-p65 (Santa Cruz, CA) (1:100 in blocking buffer) was added and allowed to incubate overnight at 4°C. Primary antibody was removed, and goat anti-mouse Alexa Fluor 488 (Molecular probes, OR) (1:1,000 in blocking buffer) was added and incubated for 1 h at room temperature in the dark. Cells were mounted with ProLong anti-fade kit as per vendor's protocol (Invitogen, Carlsbad, CA) and examined under Nikon Fluorescent microscope (Nikon, NY) at 90× magnification with oil immersion lens. The exposure time used for Alexa Fluor was 90 ms and 30 ms for PI for all the treatments. Ki-67-FITCimages were procured at 40× magnification with 47 ms exposure time for all the treatments.

Statistical Analysis

Statistical analyses of the data between treated and untreated cells were performed by Student's *t*-test. A *p*-

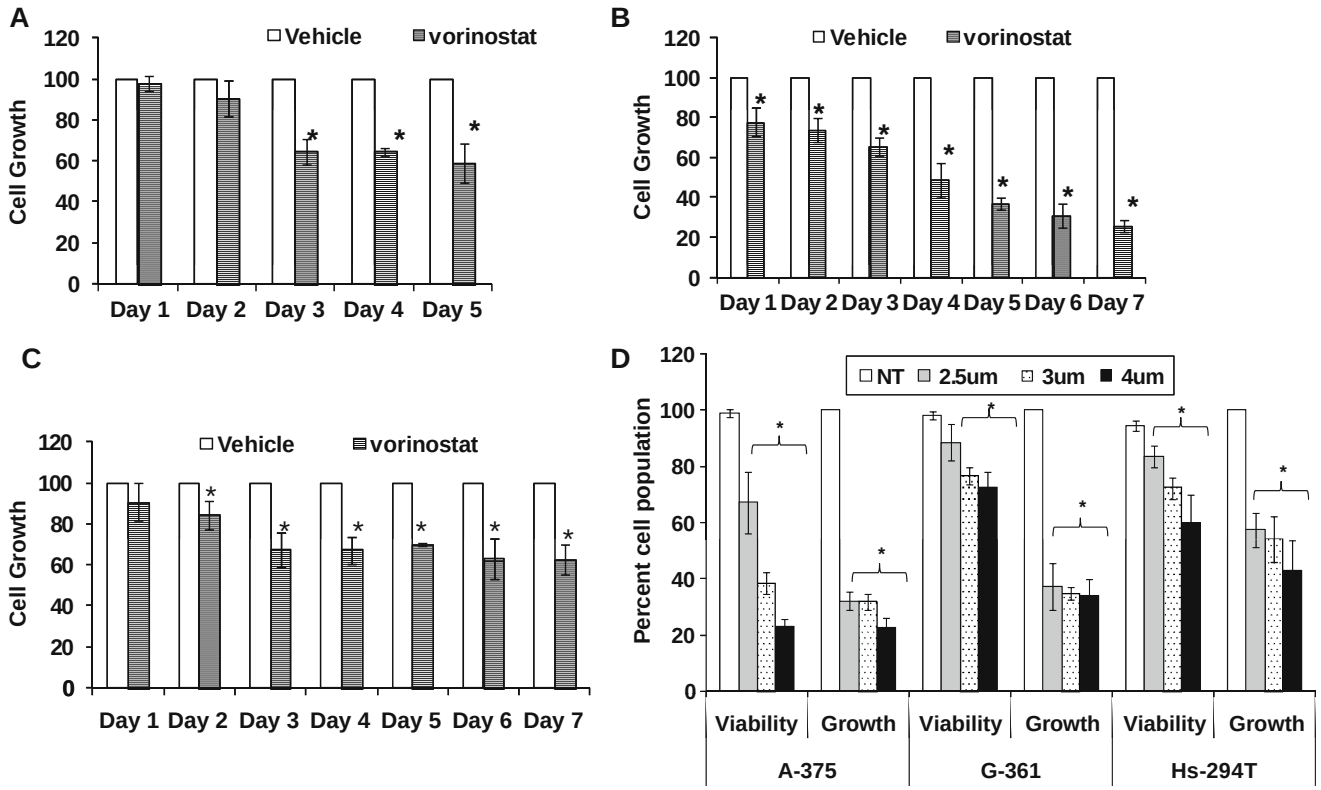

Fig. 1 Effect of vorinostat on growth of melanoma cells. (**A**) A-375, (**B**) G-361 and (**C**) Hs-294T melanoma cells (5×10^4) were treated with vorinostat (1 μM) for up to 7 days (5 days for A-375) and collected by trypsinization after each end point, washed and counted using Trypan blue analysis (no stain = viable, blue = non-viable). Cell growth was determined by counting the total number of cells and was quantitated by normalizing each treatment to its respective control. The data represent mean ± standard deviation of three experiments with similar results (*$p < 0.05$). (**D**) Dose-dependent effect of vorinostat on growth and viability of melanoma cells. Melanoma cells (1×10^5) were treated with vorinostat (2.5–4 μM) for 48 h and collected by trypsinization, washed and counted using Trypan blue analysis (no stain = viable, blue = non-viable). Cell viability was quantitated as percent viable of total cells counted. Cell growth was determined by counting the total number of cells and is quantitated by normalizing each treatment to their respective controls. The data represents mean ± standard deviation of three experiments with similar results (*$p < 0.05$).

value <0.05 was considered statistically significant. The (*) represents statistical significance compared to vehicle-treated control, EGCG (!) and to vorinostat (^).

RESULTS

Vorinostat Inhibits Melanoma Cell Growth

We first determined the antiproliferative effects of vorinostat on human melanoma cell lines, including amelanotic melanoma line A-375, melanoma G-361 and metastatic melanoma Hs-294T. The cells were treated with vorinostat at a physiological concentration (1 μM). Cellular growth was monitored for up to 7 days using the Trypan blue dye exclusion assay. Cell growth data were analyzed as the percent change of total cell numbers between controls and treatments. Vorinostat treatment reduced the growth of melanoma cells in a time-dependent fashion with the greatest response in G-361 cells, where growth inhibition from day 2 to day 7 increased from 20% to 75% ($p<0.05$). In A-375 and Hs-294T cells, growth inhibition remained steady at 30% from day 2 to day 5–7 compared to vehicle-treated control. These results demonstrated that vorinostat clearly has an anti-melanoma effect *in-vitro*. When we performed these tests at higher doses (2.5–4 μM) for 48 h, the effects on growth inhibition were even more profound (Fig. 1D).

Vorinostat Modulates the Cell Cycle and Induces Apoptosis in Melanoma Cells

Next, we determined whether the growth inhibitory effects of vorinostat were due to modulation of the cell cycle and/or apoptosis. Melanoma cells were treated with vorinostat (2.5, 3 and 4 μM) for 48 h. We found about 28% apoptotic cells (sub G1) in A-375 and Hs-294T and about 10% in G-361 using 4 μM vorinostat. All three cell lines showed an increase in the G2M subpopulation (Fig. 2). A time-dependent increase in apoptotic cells was observed at 72 h, consistent with a G2M phase arrest similar to the 48 h time point (data not shown).

Apoptotic effects of vorinostat were further investigated using annexin V binding in melanoma cell lines treated as above. A dose-dependent increase in annexin V binding from 2% to 54% was observed in A-375 treated with 1–5 μM vorinostat (Fig. 3A). G-361 exhibited about 30% apoptosis, and Hs-294T showed 33% apoptotic cell population with similar vorinostat treatment (Fig. 3B). A time-dependent increase in annexin V binding was also observed with vorinostat at 2.5–4 μM in A-375 and Hs-294T cells (Fig. 3D). At higher concentrations of vorinostat (10 μM), up to 94% apoptosis was detected in A-375 and 60% in Hs-294T, respectively (Fig. 3E), and similar results were found in G-361 cells.

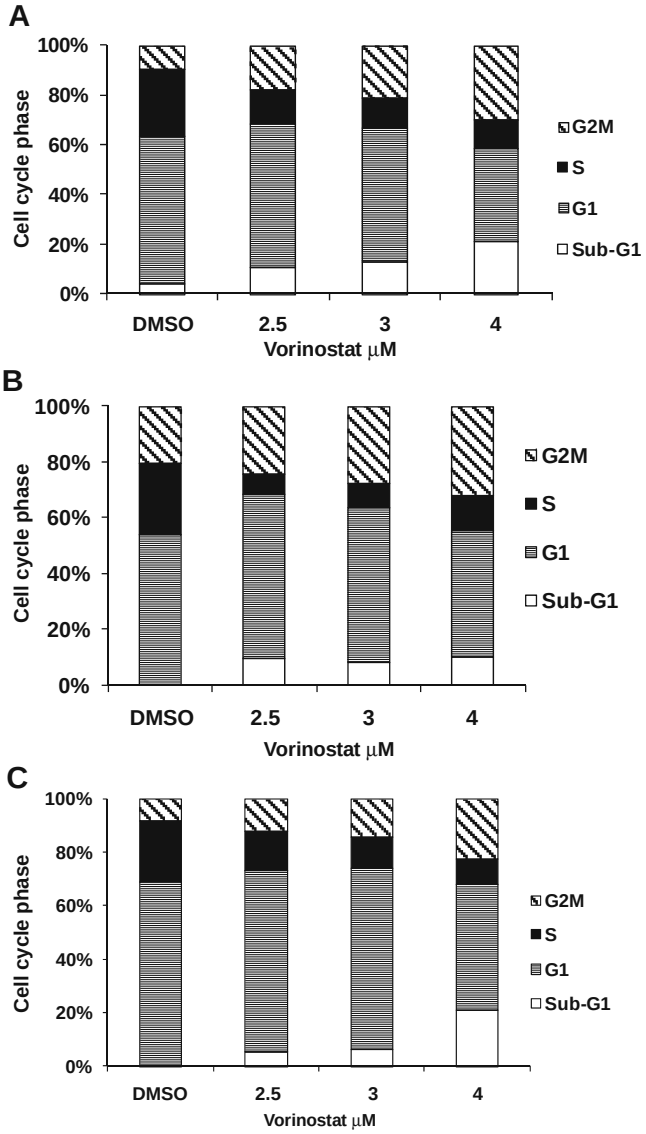

Fig. 2 Vorinostat treatment causes a G2M cell cycle arrest in melanoma cells. (**A**) A-375, (**B**) G-36 and (**C**) Hs-294T melanoma cells (1×10^5) were treated with vorinostat (2.5 μM–4 μM) for 48 h, collected and fixed for cell cycle distribution analysis using FACS. The quantitation of cell cycle distribution was performed using ModFit LT software (Verity Software House; Topsham, ME). The data represents mean ± standard deviation of three experiments (*$p<0.05$).

Combination of EGCG and Vorinostat Results in Significantly Greater Inhibition of Melanoma Growth, Clonogenic Survival and Decreased Expression of Ki-67 than Single Agents

To test the hypothesis that EGCG enhances the therapeutic efficacy of vorinostat, we treated melanoma cells with single agents and their combination to evaluate effects on proliferation. Cells were treated with vorinostat (1 μM) and/or EGCG (10 μg/mL) for 48 h, and proliferation of melanoma cells was assessed by Trypan blue exclusion. Our

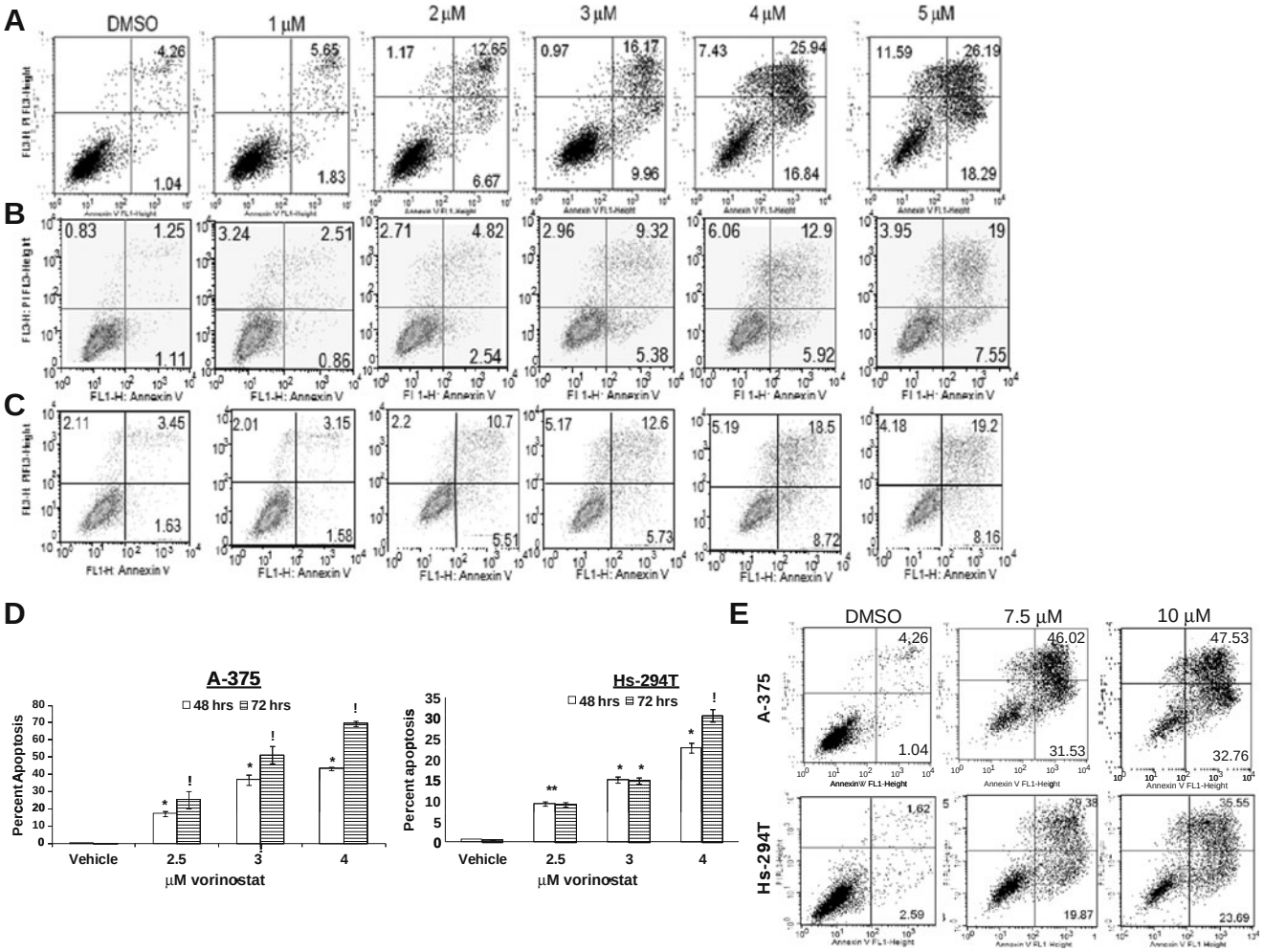

Fig. 3 Vorinostat causes apoptosis of melanoma cells. (**A**) A-375, (**B**) G-361 and (**C**) Hs-294T melanoma cells treated with vorinostat (1 μM–5 μM) in a dose-dependent fashion for 48 h. Following treatments, cells were collected, washed and stained with FITC-conjugated Annexin V antibody and PI and analyzed using FACS analysis and FlowJo software. Cells were gated and counted as viable (Annexin negative/PI negative), early apoptotic (Annexin positive/PI negative), late apoptotic (Annexin positive/PI positive), or necrotic (Annexin negative/PI positive). The dot plots represent one of three experiments with similar results (*$p < 0.05$). Time-dependent effect of vorinostat on apoptosis in melanoma cells. (**D**) A-375 and Hs-294T melanoma cells treated with vorinostat in a time-dependent fashion for 48 and 72 h. (**E**) Dose-dependent effect of vorinostat on apoptosis in melanoma cells. A-375 and Hs-294T melanoma cells treated with vorinostat in a dose-dependent fashion for 48 h.

data demonstrate that EGCG as well as vorinostat alone resulted in a modest decrease in cell viability (up to 20%) and significant growth inhibition up to 20% with EGCG and 30–60% with vorinostat (60% for A-375 and G-361, and 30% for Hs-294T). Combination treatment caused the greatest growth inhibition (65% in A-375, 70% in G-361 and 35% in Hs-294T) (Fig. 4A). There was a statistically significant cell growth inhibitory effect on G-361 and a trend for A-375 and Hs-294T (Fig. 4A).

Next, we determined the effect of EGCG and/or vorinostat treatment on clonogenic survival of the melanoma cells over 7–15 days (7 days for A-375 due to high growth), employing a colony formation assay. As shown in Fig. 4B, C and Table I, we found that EGCG and vorinostat alone resulted in a significant decrease in the number of colonies of melanoma cells, but the combination of these two agents caused a much more robust and statistically significant inhibition in the number of colonies than either agent alone.

We used immunofluorescent staining to determine the effect of these treatments on the expression of Ki-67 nuclear protein by melanoma cells. Ki-67 is expressed exclusively in proliferating cells during all active parts of the cell cycle; however, it is absent in quiescent cells and during DNA repair. Fig. 4D shows the Ki-67 FITC images. Untreated cells showed widespread nuclear Ki-67 expression. EGCG treatment resulted in reduced intensity of the FITC stain. With vorinostat and combination treatment, a few cells had a modest staining suggesting that single agents and their combination had a marked anti-proliferative effect on melanoma.

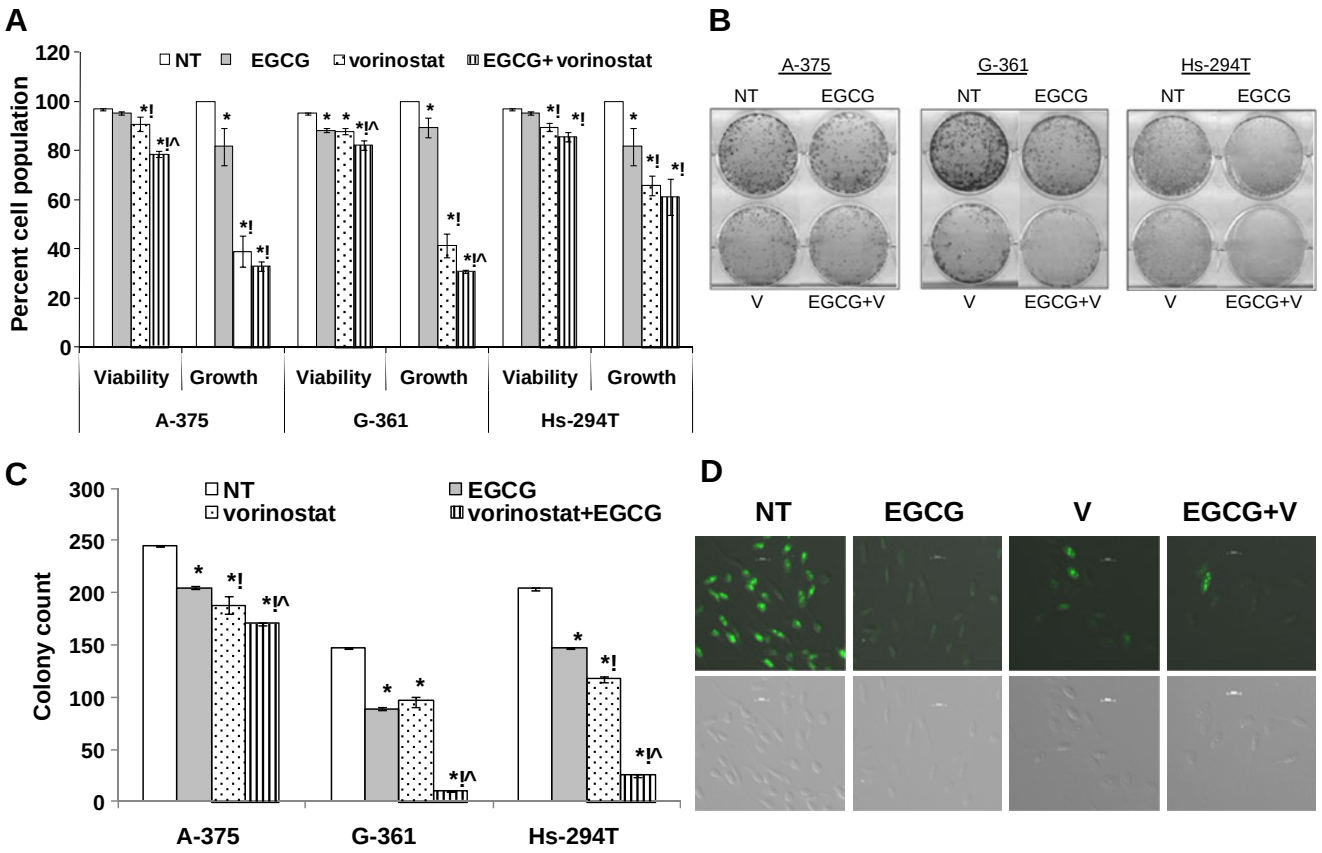

Fig. 4 Effect of EGCG, vorinostat and combination on viability, growth and colony formation of melanoma cells. (**A**) Effect of EGCG, vorinostat and combination on viability and growth. A-375, G-361 and Hs-294T (1×10^5) cells were treated with single agents and combination for 48 h, harvested and collected. The cells were counted using Trypan blue analysis (no stain = viable, blue = non-viable). Cell viability (left panels) was quantitated as percent viable of total cells counted. Cell growth was determined by counting the total number of cells and is quantitated by normalizing each treatment to their respective controls. The data represent mean ± standard deviation of three experiments with similar results. The p value ($p < 0.05$) was considered statistically significant compared with no treatment control (*), with EGCG (!), with vorinostat (^). (**B**) Effect of EGCG, vorinostat and combination on colony formation. Following treatments, A-375, G-361 and Hs-294T cells (1×10^3, 4×10^3, 5×10^3 respectively) were allowed to grow for 15 days (7 days for A-375) with media changes every 3 days. Colonies were stained with crystal violet and counted; and the data is shown as percent colony formation (normalized to control). (**C**) The data represented in histogram as mean ± standard deviation of three experiments with similar results. The p value ($p < 0.05$) was considered statistically significant compared with no treatment control (*), with EGCG (!), with vorinostat (^). (**D**) Effect of EGCG, vorinostat and combination on proliferation marker Ki-67. Melanoma cells showing marked reduction in FITC tagged nuclear Ki-67 expression in response to various treatments. Background exposure pictures show unstained cells.

Combination of EGCG and Vorinostat Results in Significantly Greater Apoptosis than Single Agents

To evaluate the effect of the combination treatment on melanoma apoptosis, A-375, Hs-294T and G-361 were treated as noted above and assessed for annexin V binding. In all three melanoma lines, combination treatment resulted in a significant increase (1.5–2 fold) in the apoptotic population relative to either EGCG or vorinostat alone (Fig. 5).

Combination of Vorinostat and EGCG Modulates Key Apoptotic and Cell Cycle Regulatory Proteins in Melanoma Cells

We found that the single agents and their combination can modulate key apoptotic and cell signaling molecules. We detected reduced proliferating cell nuclear antigen (PCNA) expression in melanoma cells with the greatest reduction due to combination treatment. PARP-1 is an abundant

Table 1 Quantitation of Colony Formation Assay Results

Melanoma cell line	NT	EGCG	Vorinostat	Vorinostat + EGCG
A-375	240 ± 4.08	205 ± 3.09*	188 ± 8.57*, [a]	170 ± 1.63*, [a]
G-361	147 ± 0.81	89 ± 7.7*	96 ± 5*	20 ± 1*, [a, b]
Hs-294T	204 ± 8.48	147 ± 3.74*	117 ± 2.60*, [a]	25 ± 1.24*, [a, b]

*$p < 0.05$
[a] with EGCG
[b] with vorinostat

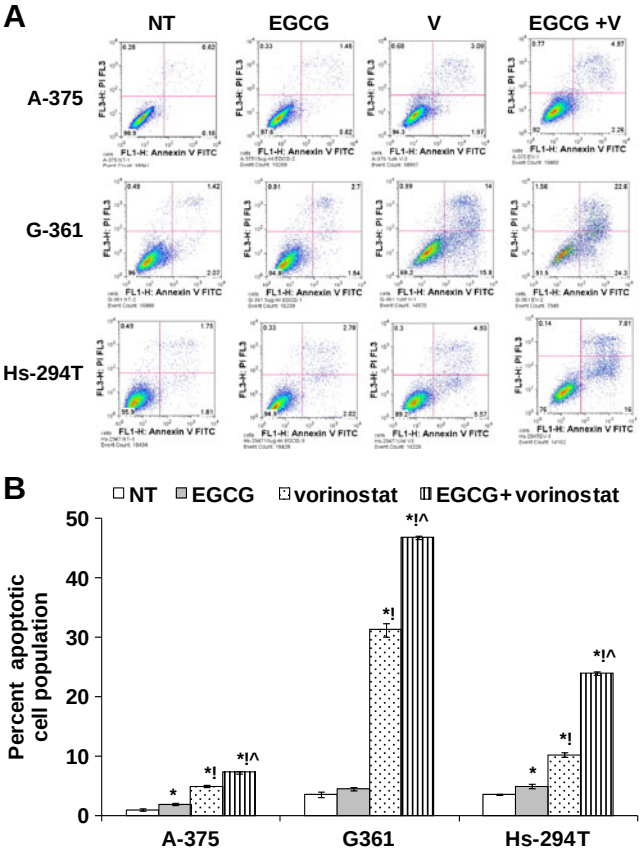

Fig. 5 Effect of EGCG, vorinostat and combination on annexin V binding. (**A**) A-375, G-361 and Hs-294T cells (6×10^3, 3×10^4, 2.4×10^4 respectively) were harvested 48 h post-treatments as stated above, collected and stained with Annexin V antibody and PI and analyzed using FACS analysis. Cells were gated and counted as viable (Annexin negative/PI negative), early apoptotic (Annexin positive/PI negative), late apoptotic (Annexin positive/PI positive), or necrotic (Annexin negative/PI positive). (**B**) Graphs represent percent of apoptotic cells (Early + Late) of total cell population. The data represent mean ± standard deviation of three experiments with similar results. The p value ($p<0.05$) was considered statistically significant compared with no treatment control (*), with EGCG (!), with vorinostat (^).

nuclear protein best known to facilitate DNA base excision repair, and its cleavage is a hallmark of apoptosis. We found decreased 119 kDa PARP and a concomitant increase in cleaved 89 kDa PARP fragment with a progressive increase from EGCG to vorinostat to combination-treated melanoma cells. We also detected the 24 kDa PARP cleavage fragment in Hs-294T and G-361 cells (Fig. 6A).

The cysteine-aspartic acid protease (caspase) family proteins play a central role in the execution phase of apoptosis. Caspases 3 and 7 are downstream factors activated by caspases 8 and 9, which in turn are activated predominantly by the extrinsic (death receptor) and intrinsic (mitochondrial) pathways, respectively. We found activation (cleavage) of caspases −3, −7 and −9 with the most cleaved protein expression induced by combination treatment (Fig. 6B). This is consistent with apoptosis mediated via the intrinsic pathway. However, we did not detect cleaved caspase 8 product in any of the treatments in melanoma cells, suggesting that extrinsic pathway of apoptosis was not triggered by these treatments (Fig. 6C).

The Bcl2 family proteins are key players in survival and apoptosis (20). Single agent and combination treatment down-regulated anti-apoptotic Bcl2 protein expression in melanoma cells where combination treatment was significantly more effective than either single agent (Fig. 6D). We next evaluated the effect of treatment on pro-apoptotic Bax. As shown in Fig. 6D, a mild overall increase in Bax protein, in conjunction with the more pronounced decrease in Bcl2, shifted the Bax/Bcl2 ratio in favor of apoptosis (Fig. 6E). Quantitative RT/PCR showed that this reduction in Bcl2 protein was due to decreased Bcl2 transcription with combination treatment causing a 60–90% reduction in Bcl2 transcript in Hs-294T and A-375/G-361 cells, respectively (Fig. 6F).

The p21 protein is a cyclin-dependent kinase inhibitor (cki) which binds to and inhibits the activity of cyclin-cdk2 or -cdk4 complexes, and thus functions as a regulator of cell cycle progression at the G1 check point. Protein p21 was induced by EGCG and vorinostat with the most expression observed in response to combination treatment in all three melanoma lines. Similarly, p27 was found to be induced with various treatments, though its induction was not as strong as p21. The treatments also down-regulated cdk2, cdk4 and cyclin A (Fig. 6G). Thus, single agent and combination therapy conferred significant changes in the protein expression of these key cell cycle regulatory molecules.

Combination of Vorinostat and EGCG Causes Down-Regulation and Decreased Activation of Nuclear Factor-Kappa B (NF-κB) p65/RelA in Melanoma Cells

In melanoma, NF-κB is constitutively activated compared to normal melanocytes (21), resulting in deregulation of gene transcription that promotes tumor cell proliferation and survival (22). Using Western blot analysis, we found that single and combination treatments were able to decrease total cellular p65/RelA expression and, as a result, nuclear p65/RelA expression as well (Fig. 7A and B).

Treatments caused reduced intensity of nuclear p65/RelA immunostaining in un-stimulated melanoma cells (Fig. 7C). At baseline, melanoma cells exhibited primarily cytoplasmic staining with the greatest nuclear staining in A-375 cells. The change in p65 intensity (orange to red) among various treatments is represented in Fig. 7D. The supplemental Fig. S1 shows NHEM, Mel1011 and Mel928 as negative and positive control for nuclear p65. The TNF-stimulated melanoma cells showed more profound treat-

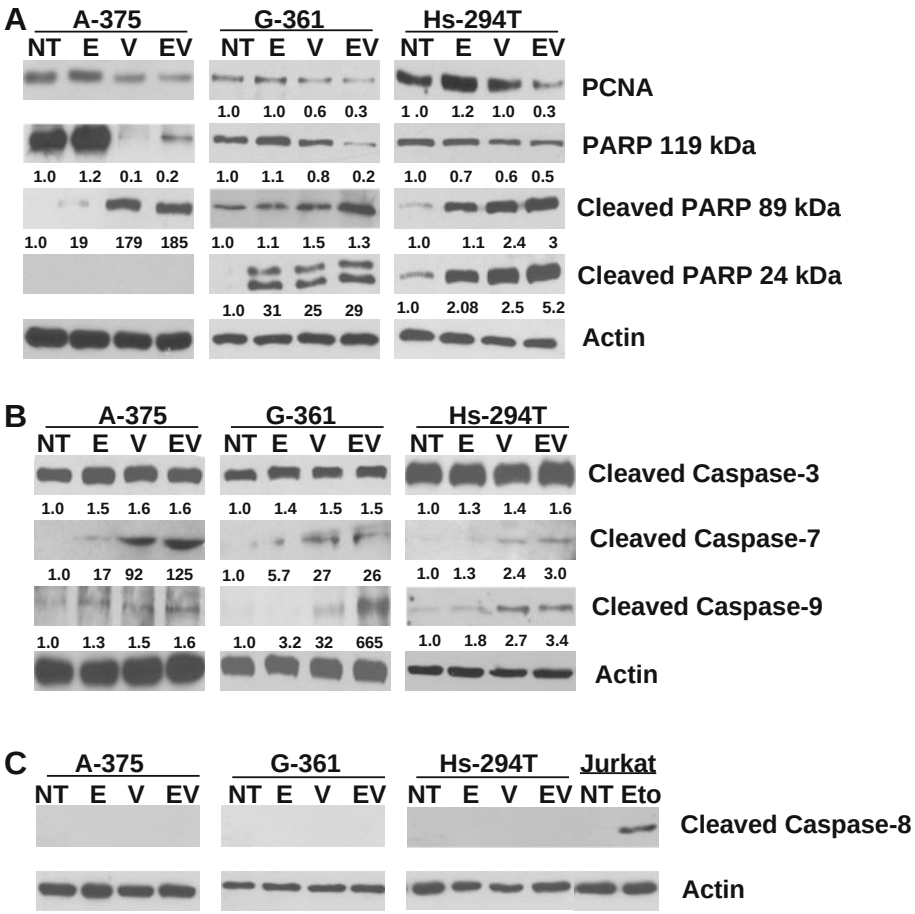

Fig. 6 Effect of EGCG, vorinostat and combination on key apoptotic and cell cycle modulatory proteins and Bcl2 transcription. Cells were collected 48 h post-treatments as stated above; whole cell lysates were prepared, and Western blot analysis was used to evaluate (**A**) PCNA, total and PARP cleavage, (**B**) cleaved caspases −3, −7, −9 (**C**) cleaved caspase-8 with etoposide-treated (25 μM for 5 h) Jurkat cells as a positive control, (**D**) Bcl2 and Bax protein expressions, (**E**) Bax/Bcl2 ratio. The data (relative density normalized to β-actin) are expressed as mean ± standard deviation of three experiments (*$p < 0.05$), (**F**) Bcl2 transcription by quantitative real time RT-PCR in melanoma cell lines. For QRT-PCR, Bcl2 mRNA levels were quantitated relative to GAPDH mRNA and calculated using the ΔΔCt method. The p value ($p < 0.05$) was considered statistically significant compared with no treatment control (*), with EGCG (!), with vorinostat (^), (**G**) cyclin-cdks-ckis protein expressions. Equal loading was confirmed by reprobing the blot for β-actin. Western blot data were quantitated by a densitometric analysis of protein bands normalized to actin.

ment responses where treatments were able to reduce the p65 intensity from yellowish-orange/orange nuclear stain to red in EGCG, vorinostat and combination group in supplemental Fig. S2. Activation of p65/RelA is associated with transport into the nucleus; therefore, our findings are consistent with a reduction in both total and nuclear p65/RelA, reflecting down-regulation of the canonical NF-κB pathway.

DISCUSSION

Melanoma is a deadly skin neoplasm that kills one person approximately every 10 min in the USA. The steady increase in its incidence, its resistance to chemotherapy and its high rate of metastasis underscore the importance of its successful prevention and treatment (1,23). Targeting key events in melanoma carcinogenesis may provide opportunities to achieve these goals (24). Previously, we showed that green tea polyphenol EGCG had cytotoxic and cytostatic effects on melanoma. The mechanism of these EGCG effects involved modulation of the cki-cyclin-cdk network and Bcl2 family proteins (5). Further, we showed that the combination of EGCG and IFN-alpha imparts a superior response in a nude mouse xenograft model of human melanoma (6).

HDAC inhibitors have proven very useful for understanding abnormal histone modification in various diseases and the role of acetylation in post-translational modification (25). HDAC inhibitors also represent a promising therapeutic option for melanoma treatment (26). Their potential synergy with other therapeutic modalities underscores the need to explore the molecular mechanisms involved (18). For example, HDAC inhibitors enhance the response of human tumor cells to ionizing radiation (17).

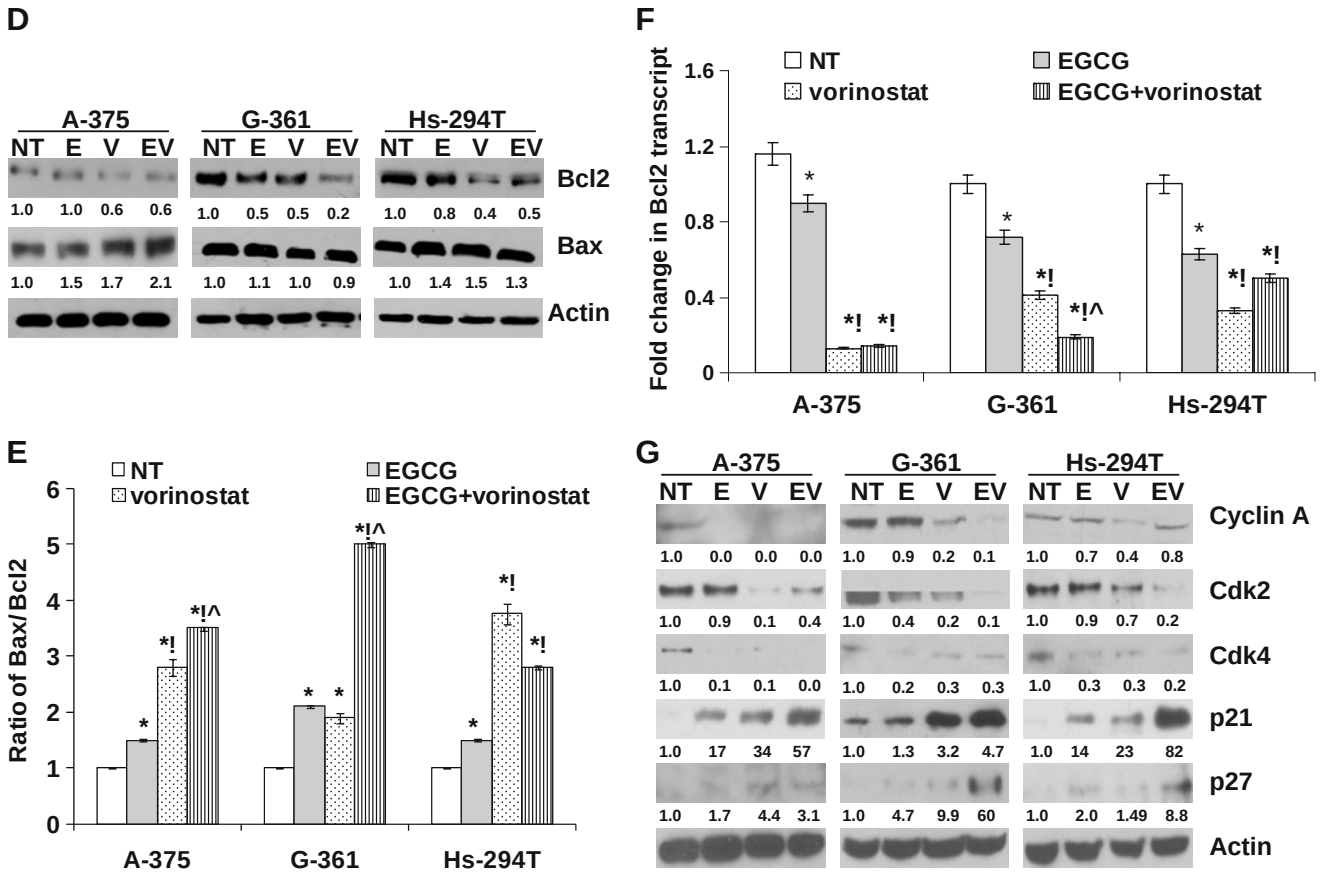

Fig. 6 continued.

Vorinostat is the first HDAC inhibitor FDA-approved for human use, specifically for the treatment of cutaneous T-cell lymphoma (11,12). Administration of Ad-hTRAIL in combination with DTIC or vorinostat enhanced apoptosis in human melanoma cell lines (27). *In vitro* and *in vivo*, the anti-tumor effect of the HDAC inhibitor LAQ824 was enhanced by combination with 13-cis-retinoic acid in two human melanoma cell lines (A2058 and HMV-I) (28). Studies of vorinostat with the proteasome inhibitor bortezomib in CTCL (29), multiple myeloma (30) and hepatoma (31) demonstrated that these two agents synergistically induce apoptosis in these tumors and thus provided a rationale for clinical trials. In the current study, we tested the anti-tumor effects of vorinostat on three human melanoma cell lines and found that vorinostat treatment resulted in inhibition of cellular proliferation and induction of apoptosis. In combination with the polyphenolic antioxidant EGCG, there was greater proliferation inhibition and increased apoptosis than with either agent alone.

Most cultured melanoma cells undergo apoptosis following treatment with HDAC inhibitors, via a mitochondrial caspase-dependent pathway (32). Our findings indicate induction of caspase 9 cleavage without appreciable effect on caspase 8. This is consistent with predominantly intrinsic as opposed to extrinsic apoptotic pathway activation. Of the many genes regulated by HDAC inhibitors, induction of p21(waf1/cip1) is the most consistent finding and is associated with G1 or G2M phase blocks (32). In T24 bladder carcinoma cells, SAHA induced up to a 9-fold increase in p21mRNA and protein, which at least in part, attributed to the rate of transcription of the gene (33). The mechanism of histone deacetylase inhibitor-activated p21gene regulation was attributed via ATM (34). Our findings with vorinostat are consistent with the literature about other HDAC inhibitors, as we found significant growth inhibition, G2M phase cell cycle arrest, p21 and p27 activation and induction of apoptosis in melanoma cells following treatment. However, the addition of EGCG further enhanced these effects, resulting in a statistically greater difference compared to either agent alone. There was greater p21 and 27 activation, proteolysis of nick sensor PARP to its stable 85 kDa fragment (an early marker of programmed cell death), activation of cleaved caspases, and down-regulation of cdk2, cdk4, cyclin A and p65/RelA. Reduction of total cellular p65/RelA is likely due at least in part to decreased transcription and is consistent with our

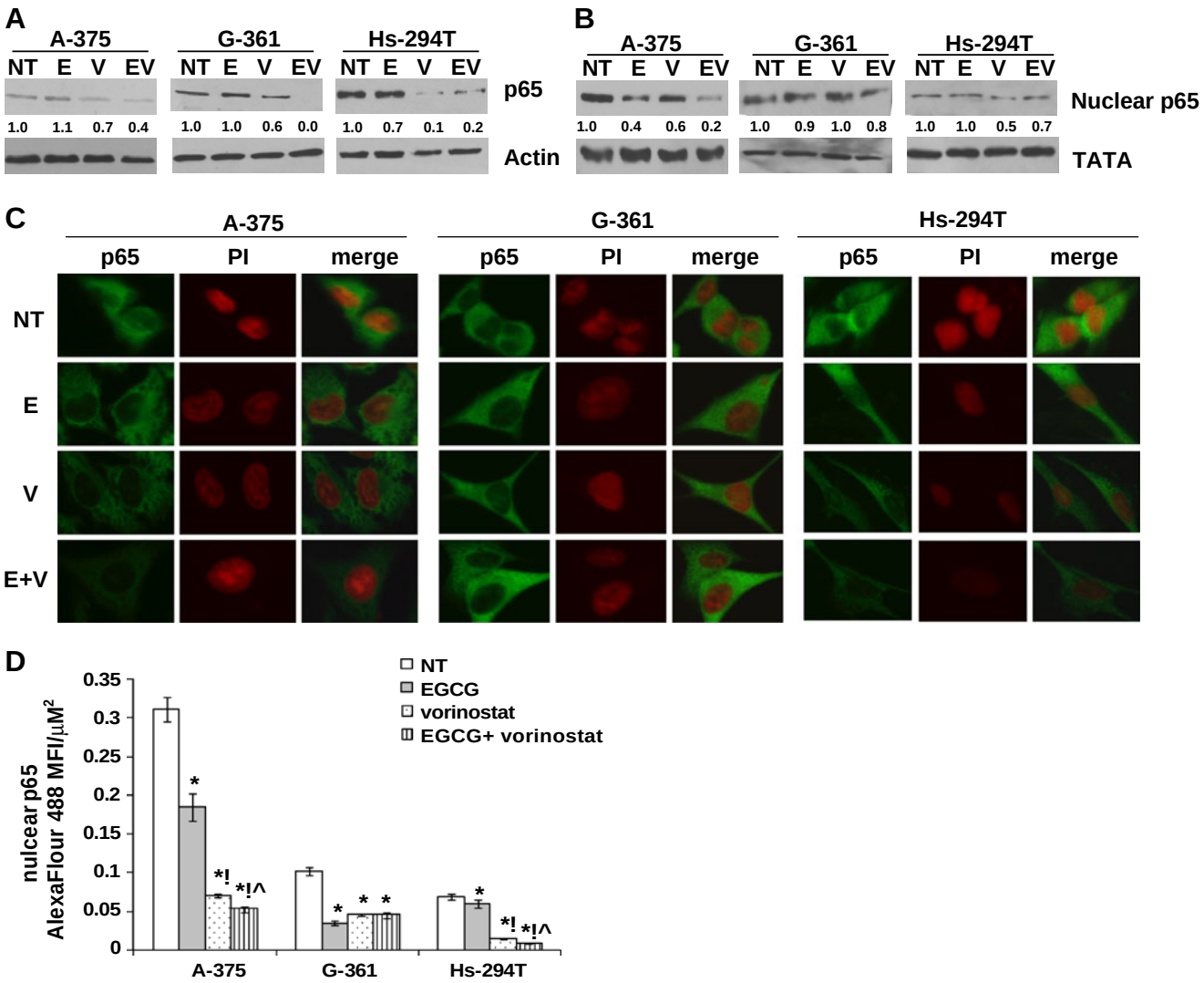

Fig. 7 EGCG, vorinostat and combination results in reduced total and nuclear expression of NF-κB (p65). (**A**) total cellular p65 and (**B**) nuclear p65 in melanoma cell by Western blot analysis as stated in Fig. 6. (**C**) Untreated and treated melanoma cells were fixed, stained for anti-p65 antibody, labeled with Alexa fluor 488 tagged secondary antibody, counterstained with PI, covered with ProLong Gold antifade reagent and analyzed by microscopy. Pictures were captured using Nikon fluorescent microscope. Representative pictures from multiple runs show NF-κB p65 (Alexa fluor 488) and DNA counterstained with PI (Red). (**D**) The ratio between change in MFI of p65 inside the nucleus/area of nucleus among treatments was plotted in the histogram. The analysis of MFI was performed using NIS software. The p value ($p < 0.05$) was considered statistically significant compared with no treatment control (*), with EGCG (!), with vorinostat (^).

prior studies showing that EGCG can down-regulate NF-κB promoter activity in melanomas (6).The quantitative variation in response to treatment among the melanoma cell lines is probably related to the heterogeneity of their signal transduction abnormalities and suggests that patient subsets may exist that will exhibit differential responses to HDAC inhibitor therapy.

Bcl2 gene family members are important determinants of apoptosis, and Bcl2 protein expression by tumors has prognostic power (20). The mechanisms by which Bcl2 family proteins regulate apoptosis are diverse. Ultimately, they govern decision steps that determine whether certain caspase family cell death proteases remain quiescent or become active (35). Therefore, it is significant that we observed that vorinostat reduced Bcl2 at both the protein and transcript levels, and shifted the Bax/Bcl2 ratio toward apoptosis. This is in contrast to studies of cutaneous T-cell lymphoma in which vorinostat treatment did not cause any change in Bcl2 expression but instead up-regulated Bax (11). However, other effects in the lymphoma cells were similar to our findings in melanoma, including up-regulated p21, activated caspases and cleaved PARP.

Acetylation of histones is regulated by HATs and HDACs which have opposing actions. Therefore, it might

seem counterintuitive that the HDAC inhibitor vorinostat and EGCG (which has HAT inhibitor activities) (36) display synergistic activity against melanoma. Nevertheless, EGCG is also an antioxidant and a demethylating agent (4,37,38). The antioxidant activity of EGCG may down-regulate pathways such as NF-κB that can be driven by reactive oxygen species (39,40). The demethylating activity of EGCG may synergize with the HDAC inhibitory action of vorinostat to help de-repress silenced tumor-suppressor genes regulating key functions such as proliferation and survival. In keeping with this view, we have shown that the combination of EGCG and vorinostat often results in greater anti-melanoma effects than either agent alone. The mechanism of these effects involves modulation of the cyclin-cdk-cki network, Bcl2 family proteins and NF-κB activity. These results provide preclinical justification for further studies exploring the potential of these agents for the treatment of melanoma patients.

REFERENCES

1. Chin L, Garraway LA, Fisher DE. Malignant melanoma: genetics and therapeutics in the genomic era. Genes Dev. 2006;20:2149–82.
2. Demierre MF. What about chemoprevention for melanoma? Curr Opin Oncol. 2006;18:180–4.
3. Demierre MF, Nathanson L. Chemoprevention of melanoma: an unexplored strategy. J Clin Oncol. 2003;21:158–65.
4. Khan N, Afaq F, Mukhtar H. Cancer chemoprevention through dietary antioxidants: progress and promise. Antioxid Redox Signal. 2008;10:475–510.
5. Nihal M, Ahmad N, Mukhtar H, Wood GS. Anti-proliferative and proapoptotic effects of (−)-epigallocatechin-3-gallate on human melanoma: possible implications for the chemoprevention of melanoma. Int J Cancer. 2005;114:513–21.
6. Nihal M, Ahsan H, Siddiqui IA, Mukhtar H, Ahmad N, Wood GS. (−)-Epigallocatechin-3-gallate (EGCG) sensitizes melanoma cells to interferon induced growth inhibition in a mouse model of human melanoma. Cell Cycle. 2009;8:1979–80.
7. Glaser KB. HDAC inhibitors: clinical update and mechanism-based potential. Biochem Pharmacol. 2007;74:659–71.
8. Duvic M, Vu J. Vorinostat in cutaneous T-cell lymphoma. Drugs Today (Barc). 2007;43:585–99.
9. Marchion D, Munster P. Development of histone deacetylase inhibitors for cancer treatment. Expert Rev Anticancer Ther. 2007;7:583–98.
10. Lee MJ, Kim YS, Kummar S, Giaccone G, Trepel JB. Histone deacetylase inhibitors in cancer therapy. Curr Opin Oncol. 2008;20:639–49.
11. Zhang C, Richon V, Ni X, Talpur R, Duvic M. Selective induction of apoptosis by histone deacetylase inhibitor SAHA in cutaneous T-cell lymphoma cells: relevance to mechanism of therapeutic action. J Invest Dermatol. 2005;125:1045–52.
12. Olsen EA, Kim YH, Kuzel TM, Pacheco TR, Foss FM, Parker S, *et al.* Phase IIb multicenter trial of vorinostat in patients with persistent, progressive, or treatment refractory cutaneous T-cell lymphoma. J Clin Oncol. 2007;25:3109–15.
13. Richardson P, Mitsiades C, Colson K, Reilly E, McBride L, Chiao J, *et al.* Phase I trial of oral vorinostat (suberoylanilide hydroxamic acid, SAHA) in patients with advanced multiple myeloma. Leuk Lymphoma. 2008;49:502–7.
14. Crump M, Coiffier B, Jacobsen ED, Sun L, Ricker JL, Xie H, *et al.* Phase II trial of oral vorinostat (suberoylanilide hydroxamic acid) in relapsed diffuse large-B-cell lymphoma. Ann Oncol. 2008;19:964–9.
15. Modesitt SC, Sill M, Hoffman JS, Bender DP. A phase II study of vorinostat in the treatment of persistent or recurrent epithelial ovarian or primary peritoneal carcinoma: a Gynecologic Oncology Group study. Gynecol Oncol. 2008;109:182–6.
16. Schaefer EW, Loaiza-Bonilla A, Juckett M, DiPersio JF, Roy V, Slack J, *et al.* A phase 2 study of vorinostat in acute myeloid leukemia. Haematologica. 2009;94:1375–82.
17. Munshi A, Tanaka T, Hobbs ML, Tucker SL, Richon VM, Meyn RE. Vorinostat, a histone deacetylase inhibitor, enhances the response of human tumor cells to ionizing radiation through prolongation of gamma-H2AX foci. Mol Cancer Ther. 2006;5:1967–74.
18. Nolan L, Johnson PW, Ganesan A, Packham G, Crabb SJ. Will histone deacetylase inhibitors require combination with other agents to fulfil their therapeutic potential? Br J Cancer. 2008;99:689–94.
19. Munster PN, Marchion D, Thomas S, Egorin M, Minton S, Springett G, *et al.* Phase I trial of vorinostat and doxorubicin in solid tumours: histone deacetylase 2 expression as a predictive marker. Br J Cancer. 2009;101:1044–50.
20. Callagy GM, Webber MJ, Pharoah PD, Caldas C. Meta-analysis confirms BCL2 is an independent prognostic marker in breast cancer. BMC Cancer. 2008;8:153.
21. Meyskens Jr FL, Buckmeier JA, McNulty SE, Tohidian NB. Activation of nuclear factor-kappa B in human metastatic melanomacells and the effect of oxidative stress. Clin Cancer Res. 1999;5:1197–202.
22. Amiri KI, Richmond A. Role of nuclear factor-kappa B in melanoma. Cancer Metastasis Rev. 2005;24:301–13.
23. Kadekaro AL, Wakamatsu K, Ito S, Abdel-Malek ZA. Cutaneous photoprotection and melanoma susceptibility: reaching beyond melanin content to the frontiers of DNA repair. Front Biosci. 2006;11:2157–73.
24. Lao CD, Demierre MF, Sondak VK. Targeting events in melanoma carcinogenesis for the prevention of melanoma. Expert Rev Anticancer Ther. 2006;6:1559–68.
25. Masuoka Y, Shindoh N, Inamura N. Histone deacetylase inhibitors from microorganisms: the Astellas experience. Prog Drug Res. 2008;66:335. 337–359.
26. Facchetti F, Previdi S, Ballarini M, Minucci S, Perego P, La Porta CA. Modulation of pro- and anti-apoptotic factors in human melanoma cells exposed to histone deacetylase inhibitors. Apoptosis. 2004;9:573–82.
27. Lillehammer T, Engesaeter BO, Prasmickaite L, Maelandsmo GM, Fodstad O, Engebraaten O. Combined treatment with Ad-hTRAIL and DTIC or SAHA is associated with increased mitochondrial-mediated apoptosis in human melanoma cell lines. J Gene Med. 2007;9:440–51.
28. Kato Y, Salumbides BC, Wang XF, Qian DZ, Williams S, Wei Y, *et al.* Antitumor effect of the histone deacetylase inhibitor LAQ824 in combination with 13-cis-retinoic acid in human malignant melanoma. Mol Cancer Ther. 2007;6:70–81.
29. Heider U, Rademacher J, Lamottke B, Mieth M, Moebs M, von Metzler I, *et al.* Synergistic interaction of the histone deacetylase inhibitor SAHA with the proteasome inhibitor bortezomib in cutaneous T cell lymphoma. Eur J Haematol. 2009;82:440–9.
30. Heider U, von Metzler I, Kaiser M, Rosche M, Sterz J, Rotzer S, *et al.* Synergistic interaction of the histone deacetylase inhibitor SAHA with the proteasome inhibitor bortezomib in mantle cell lymphoma. Eur J Haematol. 2008;80:133–42.

31. Emanuele S, Lauricella M, Carlisi D, Vassallo B, D'Anneo A, Di Fazio P, *et al.* SAHA induces apoptosis in hepatoma cells and synergistically interacts with the proteasome inhibitor Bortezomib. Apoptosis. 2007;12:1327–38.
32. Boyle GM, Martyn AC, Parsons PG. Histone deacetylase inhibitors and malignant melanoma. Pigment Cell Res. 2005;18:160–6.
33. Richon VM, Sandhoff TW, Rifkind RA, Marks PA. Histone deacetylase inhibitor selectively induces p21WAF1 expression and gene-associated histone acetylation. Proc Natl Acad Sci U S A. 2000;97:10014–9.
34. Ju R, Muller MT. Histone deacetylase inhibitors activate p21 (WAF1) expression via ATM. Cancer Res. 2003;63:2891–7.
35. Krajewski S, Krajewska M, Turner BC, Pratt C, Howard B, Zapata JM, *et al.* Prognostic significance of apoptosis regulators in breast cancer. Endocr Relat Cancer. 1999;6:29–40.
36. Choi KC, Jung MG, Lee YH, Yoon JC, Kwon SH, Kang HB, *et al.* Epigallocatechin-3-gallate, a histone acetyltransferase inhibitor, inhibits EBV-induced B lymphocyte transformation via suppression of RelA acetylation. Cancer Res. 2009;69:583–92.
37. Fang MZ, Wang Y, Ai N, Hou Z, Sun Y, Lu H, *et al.* Tea polyphenol (−)-epigallocatechin-3-gallate inhibits DNA methyltransferase and reactivates methylation-silenced genes in cancer cell lines. Cancer Res. 2003;63:7563–70.
38. Stresemann C, Brueckner B, Musch T, Stopper H, Lyko F. Functional diversity of DNA methyltransferase inhibitors in human cancer cell lines. Cancer Res. 2006;66:2794–800.
39. Cerimele F, Battle T, Lynch R, Frank DA, Murad E, Cohen C, *et al.* Reactive oxygen signaling and MAPK activation distinguish Epstein-Barr Virus (EBV)-positive *versus* EBV-negative Burkitt's lymphoma. Proc Natl Acad Sci U S A. 2005;102:175–9.
40. Fried L, Arbiser JL. The reactive oxygen-driven tumor: relevance to melanoma. Pigment Cell Melanoma Res. 2008;21:117–22.